Glycobiology vol. 17 no. 6 pp. 663–676, 2007
doi:10.1093/glycob/cwm026
Advance Access publication on March 5, 2007

Affinity of galectin-8 and its carbohydrate recognition domains for ligands in solution and at the cell surface

Susanne Carlsson[1,2], Christopher T Öberg[3], Michael C Carlsson[2], Anders Sundin[3], Ulf J Nilsson[3], David Smith[4], Richard D Cummings[4], Jenny Almkvist[5], Anna Karlsson[5], and Hakon Leffler[1,2]

[2]Section of Microbiology Immunology and Glycobiology (MIG), Sölvegatan 23, 223 62; and [3]Organic Chemistry, Lund University, 222 41 Lund, Sweden; [4]Department of Biochemistry, Emory University School of Medicine, Atlanta, GA 30322; and [5]The Phagocyte Research Laboratory, Department of Rheumatology and Inflammation Research, Göteborg University, 413 46 Göteborg, Sweden

Received on January 19, 2007; revised on February 22, 2007; accepted on February 27, 2007

Galectin-8 has two different carbohydrate recognition domains (CRDs), the N-terminal Gal-8N and the C-terminal Gal-8C linked by a peptide, and has various effects on cell adhesion and signaling. To understand the mechanism for these effects further, we compared the binding activities of galectin-8 in solution with its binding and activation of cells. We used glycan array analysis to broaden the specificity profile of the two galectin-8 CRDs, as well as intact galectin-8s (short and long linker), confirming the unique preference for sulfated and sialylated glycans of Gal-8N. Using a fluorescence anisotropy assay, we examined the solution affinities for a subset of these glycans, the highest being 50 nM for NeuAcα2,3Lac by Gal-8N. Thus, carbohydrate–protein interactions can be of high affinity without requiring multivalency. More importantly, using fluorescence polarization, we also gained information on how the affinity is built by multiple weak interactions between different fragments of the glycan and its carrier molecule and the galectin CRD subsites (A–E). In intact galectin-8 proteins, the two domains act independently of each other in solution, whereas at a surface they act together. Ligands with moderate or weak affinity for the isolated CRDs on the array are bound strongly by intact galectin-8s. Also galectin-8 binding and signaling at cell surfaces can be explained by combined binding of the two CRDs to low or medium affinity ligands, and their highest affinity ligands, such as sialylated galactosides, are not required.

Key words: affinity/cell surface/galectin/sialic acid/specificity

Introduction

The galectins are proteins defined by a carbohydrate recognition domain (CRD) with affinity for β-galactosides and a conserved sequence motif (Barondes et al. 1994; Leffler et al. 2004). The galectin CRD has about 130 amino acids, and the solved 3-D structures suggest a highly conserved β-sandwich fold, slightly bent forming a groove on the concave side. This groove forms the galectin–carbohydrate recognition site with five subsites (A–E) as depicted in Figure 1 and described in detail in Leffler et al. (2004). Subsite C interacts with β-galactose and is defining the conserved binding site shared among galectins. The other subsites define the fine specificity for larger saccharides and vary among galectin CRDs. Some galectins have one CRD and can occur as monomers, dimers, or oligomers. Other galectins have two different CRDs within the same peptide chain. Divergence from such a bi-CRD (tandem repeat) chordate ancestor (Houzelstein et al. 2004) has given rise to about 15 known mammalian galectins of both mono- and bi-CRD type.

Galectins can induce large variety of effects on many different cells (Ilarregui et al. 2005; Liu and Rabinovich 2005), giving an impression of specificity in some cases, but not in others. Many galectin activities are also overlapping. Di- or multivalency appears to be required for most of their effects on cells, and various modes of cross-linking of cell surface receptors have been proposed (Brewer 2002; Stillman et al. 2006). However, the relation between the cellular activities and the different fine specificities of galectin CRDs has only begun to be defined (Leppanen et al. 2005; Cabrera et al. 2006; Hernandez et al. 2006; Patnaik et al. 2006; Stillman et al. 2006).

Galectin-8 also has specific effects on cell signaling and adhesion (Hadari et al. 2000; Levy et al. 2001, 2006; Nishi et al. 2003; Carcamo et al. 2006), usually requiring about 10-fold less (between 0.1 and 1 μM) of added galectin compared with galectin-1 and galectin-3. The mechanism of action of bi-CRD galectins, such as galectin-8, is especially intriguing, because the two CRDs appear to differ dramatically in specificity (Hirabayashi et al. 2002; Ideo et al. 2003), but somehow act together to elicit specific effects on cells. Both domains were found to be required for many effects of galectin-8, in addition to the proper length of the linker (Levy et al. 2006). A few glycoprotein ligands, including integrins, have been identified by affinity isolation or functional inhibition by antibodies (Hadari et al. 2000; Levy et al. 2001; Nishi et al. 2003; Carcamo et al. 2006). Analysis of binding to Chinese hamster ovary (CHO) cell mutants suggested that intact galectin-8 required *N*-glycans

[1]To whom correspondence should be addressed: Tel.: +46 46-173270; Fax: +46 46-137468; e-mail: hakon.leffler@med.lu.se or susanne.carlsson@med.lu.se

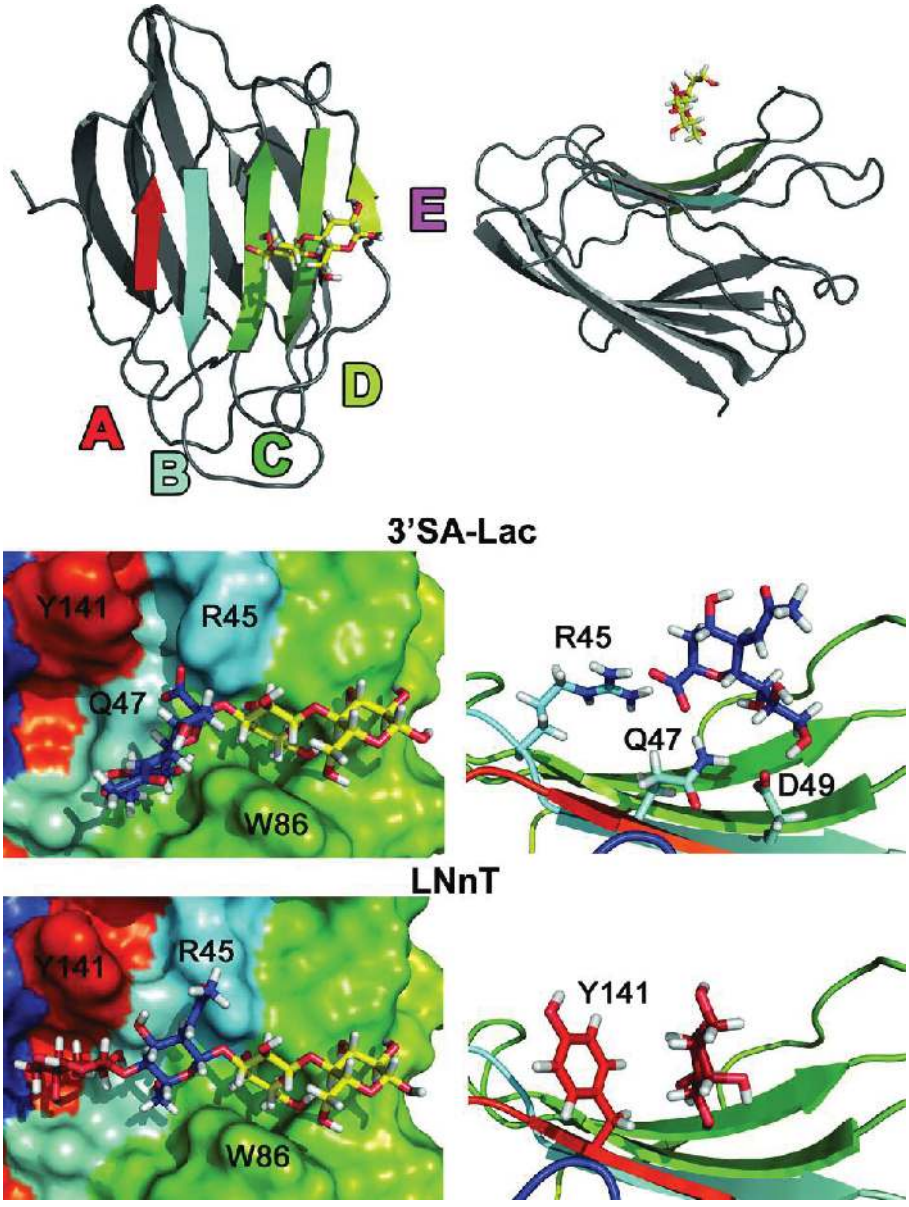

Fig. 1. Model of Gal-8N with bound ligands, 3′SA-Lac or LNnT. The top left panel shows an "en face" view of Gal-8N (ribbon model with bound lactose in yellow) with the carbohydrate-binding β-sheet in front and the corresponding carbohydrate-binding subsites (and β-strands) colored: site A (red), B (light blue), C (green), and D (greenish-yellow). Site E is the area to the right of site D. Middle and bottom left panels visualize how the two bound ligands, 3′SA-Lac and LNnT, are accommodated in the Gal-8N binding pocket (shown as a surface). The right panels show a view from the left side of the β sheets with the carbohydrate-binding groove at the top. The middle and bottom two right panels show a close up of amino acids important in the binding of each ligand. For clarity, only these amino acids together with the interacting monosaccharide are shown. Molecular graphics were generated with PyMol.

for cell surface binding (Patnaik et al. 2006). On the other hand, the best ligands for the N-terminal CRD (Gal-8N) were sialylated and sulfated lactose, as found in glycolipids but not in glycoproteins (Rauvala and Finne 1979). Thus, the relation between the CRD fine specificity and cell surface binding and signaling of galectin-8 remains unclear.

To provide a framework for understanding these issues further, we have first broadened the analysis of galectin-8 specificity using a glycan array and then addressed the following questions: What are the affinities and binding modes of each galectin-8 CRD in solution? Do the two CRDs affect each other in solution? What are the ranges of the monovalent affinity of each CRD for a cell surface? How strong cell surface binding of each CRD and how strong glycosidic cluster effects are required to explain the observed cell surface affinity of intact galectin-8 at the concentration sufficient to induce cell signaling?

Results and discussion

Galectin-8 N-terminal CRD predominantly binds α2,3-sialylated or 3′sulfated β-galactosides

A glycan array was probed with AlexaFluor488-labeled thioredoxin-fused Gal-8N (TrxG8N; Figure 2). In the figure, the glycans are ordered (and renumbered as shown in *x*-axis)

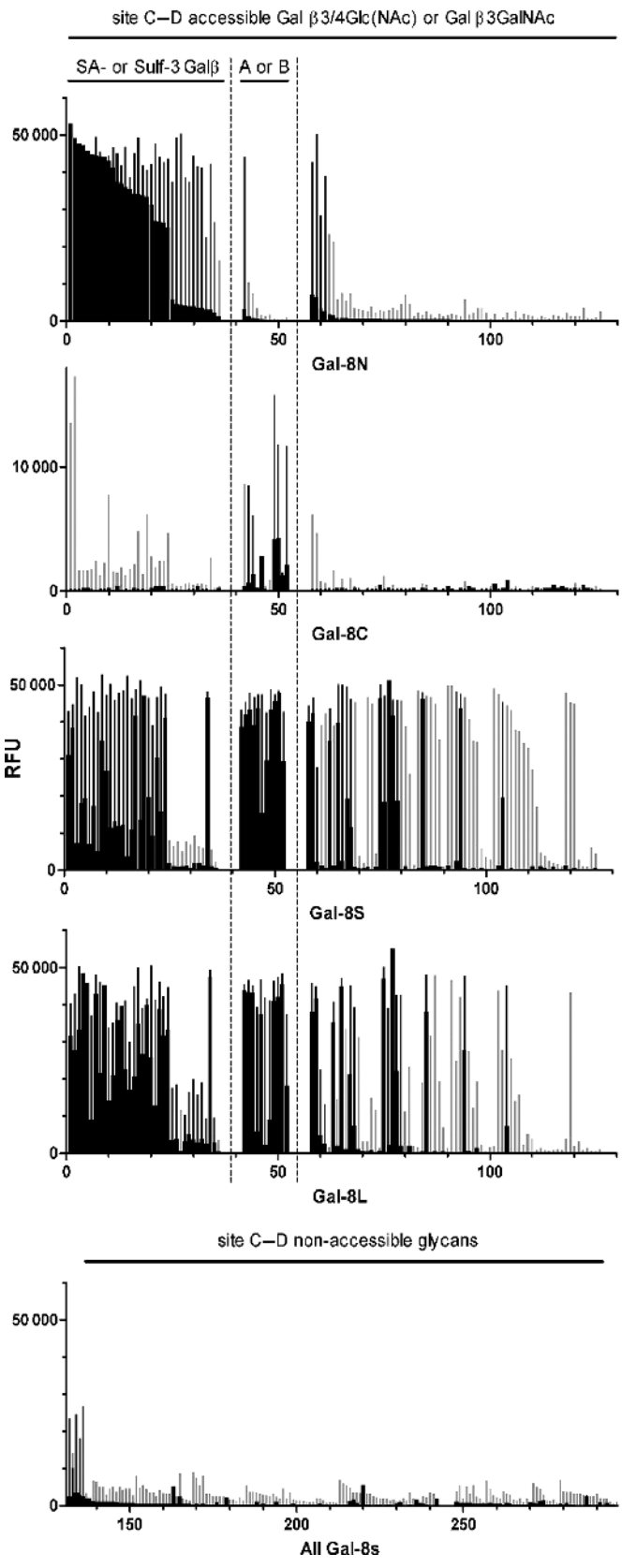

based on structural features as indicated above panels and described in legend, and data for two concentrations (low, approximately 1 μM; high, approximately 5 μM) of galectin are shown by thick black bars and by thin bars (black or gray), respectively. The bottom panel shows glycans expected, from structure, not to bind galectins, and thereby give an indication of the level of background signal (see legend to Figure 2). All data, with standard deviations, are given in Supplementary Table S1a–d, including numbering of glycans on the original array.

The strongest binding TrxG8N glycans, as seen with low (approximately 1 μM) galectin concentration (thick peaks in Figure 2), were β-galactosides with either α2,3-NeuAc or 3-linked sulfate, as previously shown by Ideo et al. (2003) and, in addition, β-galactosides with α2,3-Neu5Gc or KDN, or α2,8-elongation on the α2,3NeuAc. The preferred sialylated/sulfated β-galactoside was lactose, Galβ1-3GlcNAc, or Galβ1-3GalNAc (glycans *1–24* in Figure 2), whereas LacNAc was less preferred (e.g. glycans *26–30*) as shown by lower binding at low galectin concentration but significant binding at high galectin concentration (thin peaks). Even 6-sulfation of the Glc(NAc) or GalNAc residue in site D appears to be well tolerated, as found in the best binding glycans, *1* and *2* in Figure 2.

A few glycans without a 3-sialylated or sulfated β-galactoside gave significant binding at the high galectin concentration, such lacto-*N*-neotetraose (LNnT, *58–59* in Figure 2), which will be described further below under *Gal-8N binds a range of ligands with different affinities*, and

Fig. 2. Glycan array analysis of two forms of intact Galectin-8 (TrxG8S and TrxG8L) and its two CRDs (TrxG8N and TrxG8C). Data are shown for 277 glycans, ordered in the figure based on structural features. The top four panels (one for each galectin-8) show the glycans containing at least one β-galactoside expected to bind in sites C–D, that is the Gal in site C cannot have substitutions on positions 4 or 6, and the saccharide in site D (Glc, GlcNAc, or GalNAc) cannot have substitution on position 3 for Galβ1-4Glc(NAc) or 4 for Galβ1-3GlcNAc (Leffler et al. 2004). These saccharides are divided into three groups: the left group includes glycans, where the Galβ mentioned above has either sialic acid (SA) or sulfate (Sulf) on the position 3, the middle group includes glycans, where the Galβ is part of blood group A or B determinants (Gal(NAc)α1-3(Fucα1-2)Galβ), and the right group includes all other glycans with an available Galβ defined as above. Bottom panel shows data for all galectins (superimposed) with glycans not expected to bind, that is those not containing any galactose (248–299) and those containing one or more galactose but blocked from binding sites C–D (132–247). Arrays were probed with a low (40 μg/mL, 0.7–1.2 μM) and a high (200 μg/mL, 3.5–6 μM) concentration of each Alexafluor-tagged galectin, and signals are expressed as relative fluorescence units, RFU. The signal is saturated at approximately 50 000 RFU. The bottom panel mainly with nonbinding glycans was used to estimate a background signal of approximately 5000 RFU for TrxG8N, TrxG8S, and TrxG8L at high concentration and approximately 2000 at low concentration, and of approximately 500 for TrxG8C. The binding is shown by thick peaks for the low concentration and thin peaks (black and grey) for the high galectin concentration. Glycans binding at the high concentrations and above background at the low concentration are shown by the thin black bars. Glycans binding at the high concentration but not above background at the low, indicating some uncertainty, are shown by the thin grey bars. Within in each structural group, glycans are ordered based on their binding to TrxG8N at the low concentration. On the array, each glycan is represented by six spots, and data are reported as average RFU of four replicates after removal of the highest and lowest values. The complete list of glycans is given in Supplementary Table S1a–d with structure, number on the array, average binding, and standard deviation for each glycan.

Table I. Fluorescence anisotropy data

No.	Trivial name	Saccharide	Linker	TrxG8N		TrxG8C		TrxG8S	
				K_d	A_{max}	K_d	A_{max}	K_d	A_{max}
Lactose in subsite C–D									
1	Lactose	**Galβ1,4Glc**	L2	3.1	172	50–150	128	1.1	177
2	Lactose	**Galβ1,4Glc**	L1	1.7	186	50–150	96	1.2	151
3	3′SA-Lac	Neu5Acα2,3**Galβ1,4Glc**	L1	0.053	194	–		0.036	199
4	2′Fuc-Lac	Fucα1,2**Galβ1,4Glc**	L1	1.1	198	40	173	1.7	203
5	A-tetra	GalNAcα1,3(Fucα1,2)**Galβ1,4Glc**	L2	50–150		8.9	94	6.3	115
6	Lacto-*N*-triose	GlcNAcβ1,3**Galβ1,4Glc**	L1	16	173	46	102	8.8	163
7	LNnT	Galβ1,4GlcNAcβ1,3**Galβ1,4Glc**	L1	0.33	187	16	129	0.25	196
8	6′SA-LNnT	Neu5Acα2,6Galβ1,4GlcNAcβ1,3**Galβ1,4Glc**	L2	0.57	156	18	106	0.46	167
9	LNF-III	Galβ1,4(Fucα1,3)GlcNAcβ1,3**Galβ1,4Glc**	L2	0.24	180	20	118	0.13	187
10	LND-I	Fucα1,2Galβ1,3(Fucα1,4)GlcNAcβ1,3**Galβ1,4Glc**	L2	5.6	169	15	100	4.4	148
11	LNT	Galβ1,3GlcNAcβ1,3**Galβ1,4Glc**	L2	2.1	162	51	95	2.7	154
Lactose or Galβ1,3GlcNAc in subsite C–D									
12	2′Fuc-LNT	Fucα1,**2Galβ1,3GlcNAc**β1,3Galβ1,4Glc	L2	6.0	128	>150		11.5	121
LacNAc in subsite C–D									
13	LacNAc	**Galβ1,4GlcNAc**	L2	9.7	167	43	121	6.7	156
14	3′SA-LacNAc	Neu5Acα2,3**Galβ1,4GlcNAc**	L1	0.31	143	>150		50–150	
15	Gal-LacNAc	Galα1,3**Galβ1,4GlcNAc**	L1	50–150		16	82	23.9	108
Galβ1,3GlcNAc in subsite C–D									
16	Lacto-*N*-biose	**Galβ1,3GlcNAc**	L1	24	123	61	137	44.3	156
17	3′SA-lacto-*N*-biose	Neu5Acα2,3**Galβ1,3GlcNAc**	L1	0.14	93	>150		>150	
Galβ1,3GalNac in subsite C–D									
18	Asialo-GM_1	**Galβ1,3GalNAc**β1,4Galβ1,4Glc	L2	6.7	144	50–150	66	15.2	146
19	GM_1	**Galβ1,3GalNAc**β1,4(Neu5Acα2,3)Galβ1,4Glc	L2	4.1	136	>150		8.7	134
Nonbinding									
20	Globotetraos (Gb4)	GalNAcβ1,3Galα1,4Galβ1,4Glc	L1	–		–		–	
21	Mannose	Man	L4	–		–		–	
22	GlcNAc	GlcNAc	L3	–		–		–	
23	GalNAc	GalNAc	L2	–		–		–	
24	Chitobiose	Glcβ1,3GlcNAc	L2	–		–		–	

Estimated affinity and A_{max} of 24 different fluorescent probes to TrxG8N, TrxG8C, or TrxG8S on chilled plates (about 4 °C).

those containing lactose with a 6-sulfated glucose residue (*60–62* in Figure 2) and a blood group B tetrasaccharide (*42*).

Among the many glycans that gave a weak or no signal with TrxG8N, most were, as mentioned above, not expected to bind the galectins, i.e. those lacking galactose, or having β-galactosides with nontolerable substitutions in sites C or D (Leffler and Barondes 1986; Leffler et al. 2004) (Figure 2). A few glycans, however, gave significant, but low binding at the higher TrxG8N concentration (*132–136*): these were not random noise, but all contained 3′-sialylated or sulfated GalβGlc(NAc) as in the strongest binding glycans (*1–24*). However, the Glc(NAc) was fucosylated or Gal 6 sulfated, modifications apparently hindering binding in sites C–D, as expected. The reason why binding was not completely hindered, as for some other saccharides in the bottom panel, may be either that these modifications are partially tolerated by Gal-8N or that the spot on the array contains a low percentage of the glycans without the hindering modification, as a contaminant.

Other nonbinding glycans were β-galactosides that could potentially bind (top panel), but probably have affinity or accessibility on the array too low for the detection of TrxG8N binding at the concentrations and conditions used. These include Lac or LacNAc.

High monovalent affinity of Gal-8N built by multiple weak interactions

Fluorescence anisotropy analysis was used to measure the affinity of TrxG8N more accurately for saccharides in solution. Twenty-four fluorescein-tagged saccharide probes were tested in a direct binding assay (Table I). The best ligand for TrxG8N was NeuAcα2-3Lac linked to fluorescein with a K_d

of about 50 nM. Inhibition experiments confirmed similar K_d values for sialylated Galβ1-3GlcNAc and Galβ1-3GalNAc, but a 10 times lower affinity for sialylated Galβ1-4GlcNAc (data not shown), all in good agreement with the glycan array data. In each case, the sialylated compound bound about 100-fold better than the nonsialylated disaccharide, which explains why nonsialylated glycans did not bind on the array at the galectin concentrations tested.

To analyze how a nanomolar affinity of this monovalent interaction was achieved, the affinity of different parts of the substance (**3**) was determined (Table II), and a model of the Gal8N sialyl lactose interaction was made (Figure 1). It is clear that the affinity can be seen as being built in a stepwise fashion with β-galactose giving a K_d of about 5 mM, and then each additional moiety improving affinity by a factor of 10–100 until a K_d of 50 nM is reached (Table II). To explain this, it is useful to analyze the effects on affinity due to the addition of fragments to the ligand molecule in the simplified way described by Jencks (1981) and developed further by Murray and Verdonk (2002). The free energy difference (ΔG), governing the equilibrium when a small molecule binds a protein, can be divided into two parts: the intrinsic term (ΔG_{int}, as named in Jencks 1981 and Murray and Verdonk 2002), with a net effect to promote the interaction itself, including enthalpies of interaction, vibrational entropies, solvation effects, etc., and a counteracting term from the loss of translational and rotational entropy when the two particles (ligand and protein) become one (the complex), ΔG_{rigid} (Murray and Verdonk 2002), excluding internal motions of the particles. When a small molecule A, e.g. the galactose here, binds a protein, the free energy change can thus be described by $\Delta G_{total} = \Delta G_{Aint} + \Delta G_{Arigid}$. If a fragment B is added to A, e.g. the Glc in lactose, it will contribute to the interaction with its ΔG_{Bint}, but the ΔG_{Brigid} does not have to be included again because the molecule has already moved from solution to bound state, in other words the ΔG_{Brigid} (nearly equal to ΔG_{Arigid}) has already been "paid for" by the first interaction. Also any conformational changes of the protein that facilitates binding of B can be regarded as having been "paid for" by A.

This analysis correlates well with the general features of galectins. The interaction in subsite C is the only one strong enough to be measurable by itself and is the one which "pays" for the loss of ΔG_{rigid}. This is consistent with the tight interaction of galactose in site C via multiple hydrogen bonds and a van der Waals interaction to the conserved "galectin signature" amino acids (Lobsanov et al. 1993; Barondes et al. 1994). ΔG_{int} for this "first interaction" must be large enough to compensate for the negative ΔG_{rigid} and in addition provide for the interaction as estimated in Table II (bottom two lines). The interactions in the other subsites, by added structural fragments, do not need to pay for ΔG_{rigid} and, hence, can be much weaker and likely close to the intrinsic ΔG for each fragment (see ΔG values listed in the right part of Table II). Consistent with this, each added fragment has much fewer interactions with the galectin than seen for galactose in site C. In a built model with 3′SA-Lac (Figure 1), the ring carboxyl group of the sialic acid (SA) is situated between Arg45 and Gln47, wherefore both amino acids contribute to this interaction. In support of this, a mutation of Gln47, which is unique in this position for Gal-8N, to an alanine as found in galectin-3, decreased affinity for sialylated structures (Ideo et al. 2003; Table III). This model also shows that the C5 acetamide of Neu5Ac is directed out from the protein, explaining why the SA variants, Neu5Ac, Neu5Gc, and KDN, only differing at this position, bind equally well to Gal-8N.

Table II shows, firstly, that interaction with a single galectin's CRD can be strong enough to explain binding to glycolipids or other glycoconjugates at a surface without inferring multivalent interactions, as the affinity is in the same order

Table II. Build up of galectin-8N affinity by subsite addition

Compound	K_d (μM)	ΔG^o (kJ/mol)	ΔG^o change[d]		
			Glc	NeuAc	Linker-fluorescein
Me β-Gal	4370.00	12.6			
Lac	90.80	21.7	9.1		
Me-β-Lac	109.00	21.2	8.6		
2-Azidoethyl β-Lac	155.00	20.4			
NeuAcα2-3Lac[a]	2.70	29.9		8.2	
2-Azidoethyl β-NeuAcα2-3Lac	0.68	33.1		12.7	
Lac–linker-fluorescein	6.40	27.8			6.1
NeuAcα2-3Lac–linker-fluorescein	0.07	38.2		10.4	8.3
Estimated "rigid entropy" part[b] of ΔG^o		−15–20			
Estimated intrinsic part[c] of Gal-β-Me ΔG^o		27–33			

K_d values were determined by each compound's potency to inhibit the TrxG8N fluorescent probe interaction, and corresponding Gibbs free energy change was calculated from $\Delta G^o = RT \times \ln(K_d)$ (kJ/mol).
[a]From Ideo et al. (2003).
[b]A part of ΔG^o mainly due to loss of translational and rotational entropy upon binding, and estimated to be 15–20 kJ/mol for small molecules relatively independent of size (Jencks 1981; Murray and Verdonk 2002).
[c]The intrinsic part of ΔG^o should be total ΔG^o with the cost of the "rigid entropy" part.
[d]The change of ΔG^o due to addition of a moiety (Glc, NeuAc, or linker-fluorescein) to the ligand was calculated by subtracting the total ΔG^o for the ligand without this moiety from the total ΔG^o for the ligand with the moiety.

Table III. Relative binding abilities for TrxG8S, TrxG8S Q47A, TrxG8N, and TrxG8N Y141S to four saccharides measured by inhibition of fluorescence anisotropy with the N-CRD specific 3′SA-Lac as probe

Saccharide	TrxG8S	TrxG8S Q47A	TrxG8N	TrxG8N Y141S
Lactose	1 (195)[a]	1 (145)	1 (30)	1 (38)
3′SA-Lac	140	7.3	100	54
Lacto-*N*-triose	0.4	7.3	0.2	0.4
LNnT	4.8	87	7.1	1.9

[a]Relative binding was calculated by dividing the K_d for the protein–lactose interaction (given within parenthesis in μM) with the K_d for each of the other interactions for the same protein.

of magnitude as found for Gal-8N binding to immobilized sialo- and sulfoglycolipids (K_d values of about 20 nM) (Ideo et al. 2003). Secondly, it shows that addition of weak interaction in a multisubsite binding can have profound effects on enhancing affinity and selectivity. In the present case, interaction in the loosely defined subsite E, outside the proper binding groove (Leffler et al. 2004), with a linker-fluorescein (coupled to the saccharide in our probes) boosts the affinity by a factor of about 10. Similar interactions of the lipid part of glycolipids (Ideo et al. 2003) or the protein part of glycoproteins (Mehta et al. 1998; Somers et al. 2000) can easily achieve the same.

Gal-8N binds a range of ligands with different affinities

Even if Gal-8N has a strong preference for glycans with 3′-sialylated or sulfated terminal galactose residues, fluorescence anisotropy analysis showed that it also binds well to saccharides not containing these structures, with measurable affinities ranging from K_d approximately 240 nM to over 50 μM. The binding to the best nonsialylated ligand, LNnT, was also detected on the array when 5 μM galectin was used (*58–59* in Figure 2, top panel). Detection of binding to additional saccharides by fluorescence anisotropy, which were not seen on the array, is possible because much higher galectin concentrations can be used, and because the fluorescein tag may enhance the affinity of some saccharides (Table II).

To explain the broad specificity of Gal-8N, we analyzed the way by which the saccharides are bound in this lectin with fluorescence anisotropy analysis. The monosaccharide residues of each saccharide that is most likely in subsites C–D (the core binding site) of the galectin are marked in bold in Table I. Thus, residues extending from these at the nonreducing side (to the left of the bold part) will be located in sites A–B and those at the reducing side (to the right of the bold part) will be projected into site E and beyond. One part of evidence for this is structural. Thus, if the saccharide contains only one β-galactose, it is most likely bound in site C. If the saccharide contains two β-galactoses, one can be assumed to be in site C if the other is hindered by substitutions that would block binding there, as explained above (e.g. 3′Fuc in **9** and 6′NeuAc in **8**) (Leffler, and Barondes 1986; Leffler et al. 2004).

Another part of the evidence for how the saccharides are binding comes from the A_{max} values measured by fluorescence anisotropy analysis. A_{max} values depend on the local environment of the fluorescein of a bound probe and hence give information on how the saccharide is bound to the galectin. A_{max} for probes **7**–**11** are high (>150 mA, Table I) and for most similar to **1**–**4** and **6**. Had TrxG8N bound the terminal LacNAc of e.g. **7** in site C–D, a much lower A_{max} would have been expected, as the internal lactose then would have put the fluorescein farther away and, hence, made it more mobile. By analogous arguments, probes **18** and **19** must bind with their terminal Galβ1-3GalNAc in site C–D since the internal lactose is blocked by the 4′GalNAc, consistent with a relatively low A_{max}.

In conclusion, the subsites A–D of Gal-8N can accommodate several saccharides, having various effects on the affinity. They either enhance the affinity (as SA in site B or LacNAc in A–B) or are tolerated (as GlcNAc or Fuc in site B, or 6′SA-LacNAc in site A–B). High specificity may be used for the selection of desired cell surface ligands positively, whereas tolerance may be needed to overlook naturally occurring individual differences, e.g. blood group determinants. The importance of this phenomenon is yet not established.

A model of Gal-8N with LNnT was built (Figure 1, bottom panels) to explain how this saccharide could be accommodated with its Lac residue in sites C–D, and how it could have almost as high affinity as 3′SA-Lac. LNnT adopts a conformation similar to its solution structure (Landersjo et al. 2005) and its crystal structure in complex with galectin-3 (J. Seetharaman et al., unpublished data). The Gln47 of Gal-8N apparently makes the interaction in site B with GlcNAc less favorable since lacto-*N*-triose (LNT) has relatively low affinity (Table III), which is higher in the Gln47Ala mutant. However, the less favorable binding of GlcNAc may be compensated by a more favorable stacking interaction of the terminal Gal with Tyr141, of a type frequently found in Gal interaction with many proteins (Rini 1995). In support of this, the affinity of LNnT was significantly lower for a Tyr141Ser mutant (Table III).

Carbohydrate specificity of the C-terminal CRD

The C-terminal CRD (TrxG8C) gave much weaker signals on the array, with its strongest signal for the best ligand being only about 30% of the maximum relative fluorescence units (RFU) at high galectin concentration (Figure 2, second panel). Part of the reason for the lower signal is lower specific labeling of TrxG8C, but part is also lower affinity. The latter is shown by approximately 5-fold difference in binding between low and high concentration of the lectin even for the best ligand, demonstrating that binding was not saturated at the concentrations used. The three best saccharides all contained the blood group A determinant GalNAcβ1-3(Fucα1-2)Gal- on either a LacNAc or Galβ1-3GlcNAc core, and binding was also found for some saccharides with blood group B determinant [Galα1-3(Fucα1-2)Gal-] [bars in middle group (marked A or B) of Figure 2]. Possible binding was also indicated, at higher galectin concentrations, for LNnT (*58–59*, Figure 2), for some saccharides with two sulfate groups or NeuAc (**1**, **2**, **10**, and **19**), and for sialylated saccharides with a second nonsialylated internal β-galactoside that was able to bind site C–D (**17** and **24**). The binding to these saccharides is, however, uncertain, since there was no binding at the 5-fold lower galectin concentration. Analysis of fluorescence anisotropy data as described for TrxG8N (Table I) showed that TrxG8C had significant measurable solution affinities in the range approximately 10–100 μM for our collection of probes. Binding was abolished by NeuAcα2-3 (**3**), but enhanced by Galα1-3 (**15**, K_d 15.5 μM) or GalNAcα1-3(Fucα1-2) (**5**, K_d 8.8 μM), in agreement with array data. Analogous to the N-CRD, bold disaccharides in Table I bind in sites C–D.

The specificity of intact galectin-8 is additive in solution but synergistic to surface bound glycans

In fluorescence anisotropy analysis, the pattern of binding for TrxG8S is dominated by the overall stronger affinity of the N-terminal CRD to most probes (Table I). For these probes, the affinity and A_{max} values with the intact galectin-8 are not significantly different from the ones with TrxG8N. Moreover, the IC_{50} for lactose inhibition is the same as for

TrxG8N (not shown). Conversely, probes **5** and **15** that bound TrxG8C better than TrxG8N also bound intact galectin-8 with about same affinity and A_{max} as found for TrxG8C, and now IC_{50} for lactose inhibition of this interaction was the same as with TrxG8C. In conclusion, the two domains in intact galectin-8 act independent of each other in solution with about the same specificity and affinity as the isolated domains.

On the array, TrxG8S bound a pattern of saccharides that is the sum of those bound by either domain with many additional saccharides (Figure 2, third panel). The binding to the latter is apparently mediated by the combined binding of the two CRDs, even if the binding of each CRD by itself is too weak to be detected on the array under the present conditions. In support of this, for example, the saccharide of probe **12** (Table I), which showed moderate or low, but significant, affinity to both CRDs in fluorescence anisotropy analysis, bound the intact galectin-8 the best on the array (*77* and *78* in Figure 2), but not either CRD by itself. The saccharides binding intact galectin-8 (near saturation at lower concentration, indicating $K_d \geq 1$ μM, Supplementary Table S1c) and not binding either CRDs well, all had at least two repeated β-galactosides selected from Lac, LacNAc, or Galβ1-3GlcNAc (e.g. **34** and **75**).

The enhanced bivalent interaction of intact galectin-8 with the array would represent a glycoside cluster effect (Rini 1995; Lee and Lee 2000; Collins and Paulson 2004; Kiessling et al. 2006) and can be analyzed in an analogous way as for the binding of a molecule to the different CRD-subsites described above under *High monovalent affinity of Gal-8N built by multiple weak interactions*. Now $\Delta G_{Atotal} = \Delta G_{Aint} + \Delta G_{Arigid}$ would represent the surface binding of one CRD, and an additional binding by the second CRD would contribute only with its ΔG_{Bint}. If the preformed spacing of the CRD-binding sites matches the preformed spacing of the surface ligands perfectly, a maximum cluster effect would be obtained with K_d (in M) close to the K_d of one CRD–ligand pair times the K_d of the other(s) and increased further by a factor corresponding to the "saved" ΔG_{Brigid}. For hepatic C-type lectin, for example, a monovalent interaction with K_d in mM range was enhanced to K_d in μM range for a bivalent interaction, and K_d in nM range for a trivalent interaction (Lee et al. 1983). If the preformed CRD and ligand spacings do not match, they may be able to adapt to each other by movements, paying in energy. For galectin-8, a far less than maximum cluster effect suffices to explain the best binding to the array. For example, compound **12**, the saccharide of which gave the best binding of intact galectin-8 to the array, had an affinity for N-terminal CRD of 6 μM. Then the other CRD needs only to push the combined affinity by a factor of about 10, which would require only a very weak net affinity for itself (compare Table II and the discussion above under *High monovalent affinity of Gal-8N built by multiple weak interactions*).

Binding of galectin-8 to cells is mediated by second best ligands of moderate affinity

From the discussions in the previous section, it can be concluded that the two CRDs of galectin-8 act independently in solution, but at a surface they can act together to achieve high-affinity binding to saccharides not bound well by either CRD alone. The same appears to occur at the cell surface as examined by measuring the binding of fluorescein-labeled galectin to U937 cells (Figure 3) and MOLT-4 cells (not shown). At 0.2 μM, both F-TrxG8L and F-TrxG8S showed a strong binding to the cells, whereas the single CRDs bound poorly (Figure 3A) and their binding could only be seen at higher concentrations (bottom panels of Figure 3B). The binding was specific and carbohydrate-dependent, because fluorescein-labeled thioredoxin did not bind cells and binding of all four galectin-8 variants could be inhibited by 100 mM lactose (data not shown).

For intact galectin-8, the binding increased linearly with increasing concentrations of galectin (Figure 4A). However, concentrations above 1 μM could not be tested as the cells started to agglutinate. The linear increase could be due to the presence of multiple receptors of different affinity in the range from K_d approximately 10 nM to several micromolar concentrations. Alternatively, as a theoretical extreme, it could be mainly due to high-affinity receptors (e.g. $K_d <$ 10 nM), in such large numbers that they were not saturated by the added galectin. To distinguish these possibilities, the dose–response of the lactose inhibition of the binding of 0.2 μM galectin was compared with theoretically calculated inhibition curves assuming different K_d values and receptor numbers (Figure 4B). The data points fell slightly above and below the curve, representing an average receptor affinity of approximately 50 nM and approximately 15 million receptors. The data clearly did not agree with much higher affinity receptors present in larger numbers. The accuracy of the analysis cannot exclude lower affinity receptors in larger numbers. Thus, the binding data for intact galectin-8 to U937 cells are most consistent with the presence of multiple receptors of affinity $K_d > 10$ nM, and probably ranging to micromolar concentrations. Such affinities can easily be achieved by the binding of each CRD to the second best ligands of moderate affinity ($K_d > \sim 1$ μM) combined with a moderate glycosidic cluster effect, as discussed in detail in *The specificity of intact galectin-8 is additive in solution but synergistic to surface bound glycans*.

The data for TrxG8N and TrxG8C, with very low binding at 0.2 μM (Figure 3A) and 100 and 50 times more binding at 2 and 4 μM, respectively (Figure 3B, bottom panels), suggest multiple receptors with affinities above 200 nM, and for most above 1 μM. This was also supported by the dose–response of lactose inhibition of the binding of 2 μM Gal-8N, with IC_{50} of approximately 0.5 mM (not shown) by the same argument as given for intact galectin-8 above. This shows that the monovalent affinities measured in solution (Table I) are sufficient to explain most cell surface binding of Gal-8N and Gal-8C.

Since the preferred ligands for Gal-8N in solution contain NeuAcα2-3Gal, we examined the role of SA at the cell surface for galectin-8 binding. Cells were treated with either a nonlinkage-specific neuraminidase (NA), cleaving all common linkages for SA, or an α2,3-linkage-specific one. The expected effect was confirmed by decreased binding of the SA-binding lectins *Sambucus nigra* agglutinin (SNA) and/or *Maackia amurensis* lectin (MAL) II (not shown). As expected, treating the cells with both NAs reduced binding of TrxG8N by approximately 90% (Figure 3B), showing that most of the Gal8N receptors contain α2,3-linked SA. In contrast, TrxG8C bound much

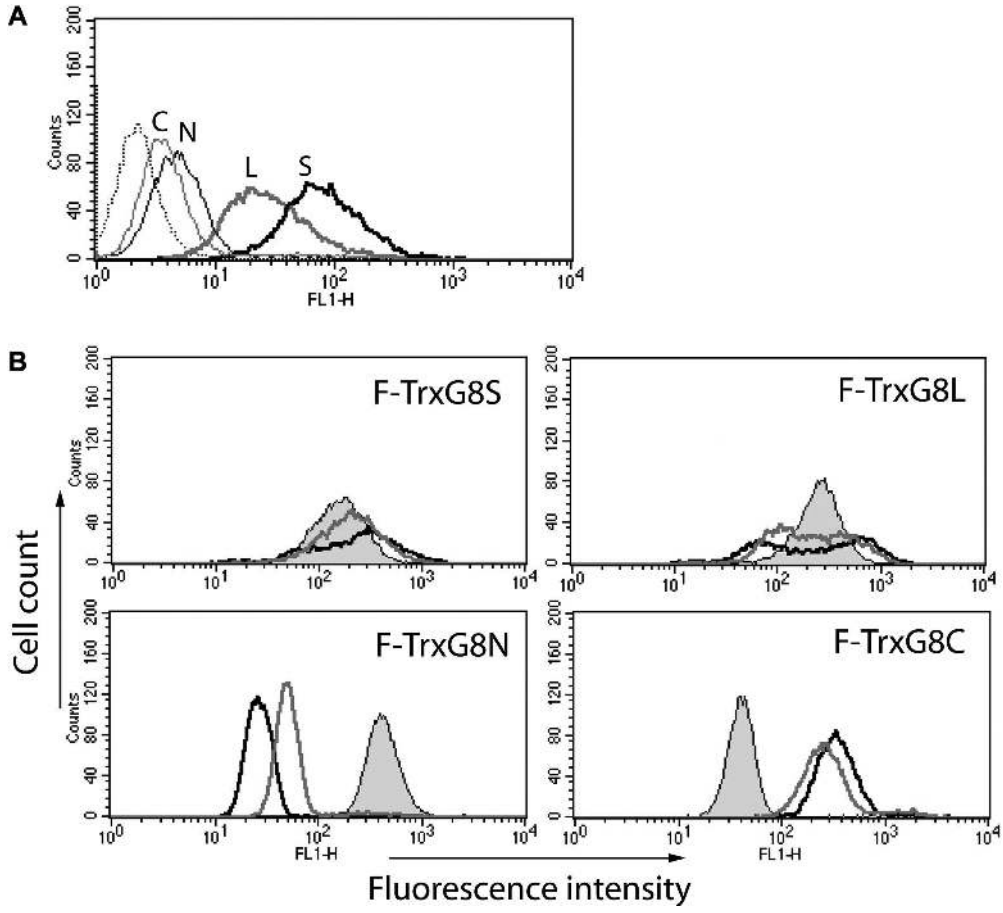

Fig. 3. Galectin-8 cell surface binding. (**A**) Flow cytometry analysis of U937 monocyte cell line incubated in the presence of 0.25 μM fluorescein-labeled galectin-8 proteins: F-TrxG8S (thick black line), F-TrxG8L (thick dark grey line), F-TrxG8N (thin black line), or F-TrxG8C (thin dark grey line). Dashed line represents unlabeled cells. (**B**) Binding of F-TrxG8L (0.2 μM), F-TrxG8S (0.2 μM), F-TrxG8N (2 μM), or F-TrxG8C (4 μM) to untreated (closed histogram) or NA treated U937 cells (open histograms). Two NAs were used, NA from *V. cholerae* (VC-NA, black line) and recombinant 2,3-specific (2,3-NA, dark grey line).

more to NA-treated cells compared with nontreated, control cells, in accordance with its specificity in solution.

The average binding of the intact galectin-8s (TrxG8S and TrxG8L) changed little after NA treatment of the cells, although the spread increased (Figure 3B, top panels). The average affinity of the NA-treated cells was very similar to that found for the untreated cells, as estimated from the lactose inhibition curve (Figure 4). An analogous result was obtained with mutant CHO cells lacking NeuAc at their cell surface, which had decreased binding of Gal-8N, but similar binding of intact galectin-8 compared with the wild-type cell (Patnaik et al. 2006). These results indicate that nonsialylated ligands may also provide sufficient affinity for intact galectin-8 to cells, even if they do not do so for the N-terminal CRD, as was found for binding to the artificial surface of the glycan array. Moreover, the Q47A mutant of TrxG8S, with decreased affinity for α2,3-sialylated galactosides (Table III), did not bind significantly different to the cells compared with wild type (not shown). Here, the mutant's increased affinity for GlcNAc-substituted galactosides, suggested by the data for LNT and LNnT (Table III), might also have compensated. In summary, the most preferred ligands of Gal-8N are not necessary for cell surface binding of intact galectin-8.

Activation of the NADPH-oxidase in neutrophil leukocytes requires intact galectin-8 but not the high affinity for sialylated galactosides

To relate the biological activity of galectin-8 to its solution affinities and cell surface binding, we wanted to examine the ability and concentration of galectin-8 required to elicit a signal in cells. We used oxidative burst in primed neutrophil leukocytes as experimental setup, a system studied extensively by us before regarding galectin-1 and galectin-3 (Karlsson et al. 1998; Almkvist et al. 2001, 2002). Neutrophils were purified from peripheral blood and primed (with LPS or TNFα) and activated by the addition of galectin, whereafter the production of superoxide anions were measured both intracellularly (a result of activation of NADPH-oxidase situated in the membrane of specific granules) and extracellularly following activation of NADPH-oxidase sitting in the plasma membrane (Figure 5). The separate CRDs only activated low production of oxygen species at concentrations above 5 μM (Figure 5). For the intact galectin-8s, responses were clearly visible already at 0.5 μM and reached their maximum between 1 and 2.5 μM. The extracellular response differed between long and short isoforms of galectin-8, because

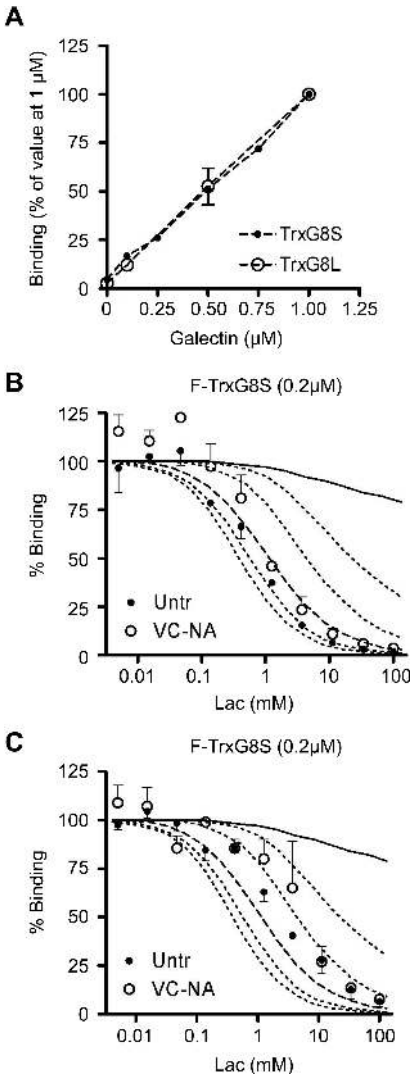

Fig. 4. Dose–response of cell surface binding by galectin-8 and of its inhibition by lactose. (**A**) Relative binding of 0.1–1 μM F-TrxG8S (•) and F-TrxG8L (○) to U937 cells. Binding of 1 μM is 100%. (**B**) Binding of F-TrxG8S (0.2 μM) and F-TrxG8L (0.2 μM) to U937 cells in the presence of increasing concentrations of lactose, for untreated cells (untr, •) and *V. cholerae* NA-treated cells (VC-NA, ○). Theoretical lactose inhibition curves (broken lines) were calculated for average cell surface affinities of $K_d = 3$, 10, 50 (dashed), 300, and 1000 nM (from left to right) and assuming approximately 15 million receptors per cell. The continuous line on top is calculated for 100 million receptors per cell of affinity $K_d = 10$ nM.

TrxG8S activated plasma membrane NADPH-oxidase with about 1.5 times higher maximum response and about 5 times higher potency (for equivalent response) compared with TrxG8L. However, for the intracellular NADPH-oxidase activation, there was no difference between the two galectin-8 isoforms. In summary, both CRDs linked together are needed to induce intra- and extracellular oxidative bursts in primed neutrophils. The required concentration is similar to that reported for other effects of soluble galectin-8 (50–500 nM), and about 10–100-fold lower than reported for effects of galectin-3 and galectin-1.

To test the role of SA, we could not use NA treatment of neutrophils as this causes complex effects on priming and activation (Almkvist et al. 2004). Instead, the results above were compared with those found for the SA-binding deficient Gln47Ala mutant galectin-8S (Table III). The dose–response of this mutant did not differ much from that for wild-type galectin-8S (Figure 5B, left panel), although it might be slightly less potent especially for induction of extracellular release of superoxide anions. The curves for inhibition of neutrophil activation by lactose were also very similar (Figure 5B, right panel). As mentioned earlier for lactose inhibition of galectin binding (Figure 4B), these curves would be expected to change if there was a major change in receptor affinities and/or numbers. Thus, the data indicate that the strong SA-binding ability of Gal-8N does not play a major role in the neutrophil activation by the intact galectin-8.

Conclusions and perspectives

The present results demonstrate that the galectin-8 N-terminal CRD can have very high monovalent affinity for sialylated or sulfated galactosides, enough to explain the binding of this CRD to the cell surface without inferring multivalency. However, the N-terminal CRD also binds various nonsialylated or sulfated saccharides with a wide range of lower affinities. These affinities are sufficient for the N-CRD to act in concert with the C-CRD to bind cell surfaces and induce signals. Thus, it appears as if galectin-8 has a relatively broad specificity for cell surface binding and signal induction, which may be functionally important, but a much more narrow preference and high affinity for the monovalent interaction with sialylated/sulfated galactosides, which is unique among mammalian galectins.

The broad specificity of galectin-8 is not unspecific as it requires β-galactosides that able to interact with the galectin core site C, but it does not depend on the further fine specificity. Some effects of other galectins may also be of this relatively "broad" type, based on interaction with ligands of moderate affinity. For example, various constructs of the bi-CRD galectin-9 containing either two N-CRDs or two C-CRDs had similar cell surface binding and activities as the wild type (Lu et al. 2007), indicating that a precise combination of the natural fine specificities was not required. Some of the many overlapping activities of galectin-1 and galectin-3 (Ilarregui et al. 2005; Liu and Rabinovich 2005; Patnaik et al. 2006) may also be of this type, and not depend on the fine specificities that distinguish each of these galectins; thus, binding to lower affinity ligands could be biologically relevant.

The biological role of the fine specificity of galectin-8, i.e. preference for sialylated and sulfated glycans, remains unknown. Most recently we found, however, that it determines the intracellular pathway of galectin-8 after endocytosis (Carlsson, Carlsson, and Leffler, unpublished). Thus, the function may be related to that suggested for galectin-4 in targeting to lipid rafts (Delacour et al. 2005; Danielsen and Hansen 2006) or galactin-3 in apical targeting of vesicles (Delacour et al. 2007). Galectin-8 fine specificity may also determine binding to selected cell types with much higher affinity, and perhaps other effects, than those so far observed. Or maybe only one CRD has to provide the affinity for one cell surface, to leave the other open for interaction with another cell or extracellular matrix? Finally, the possibility that each

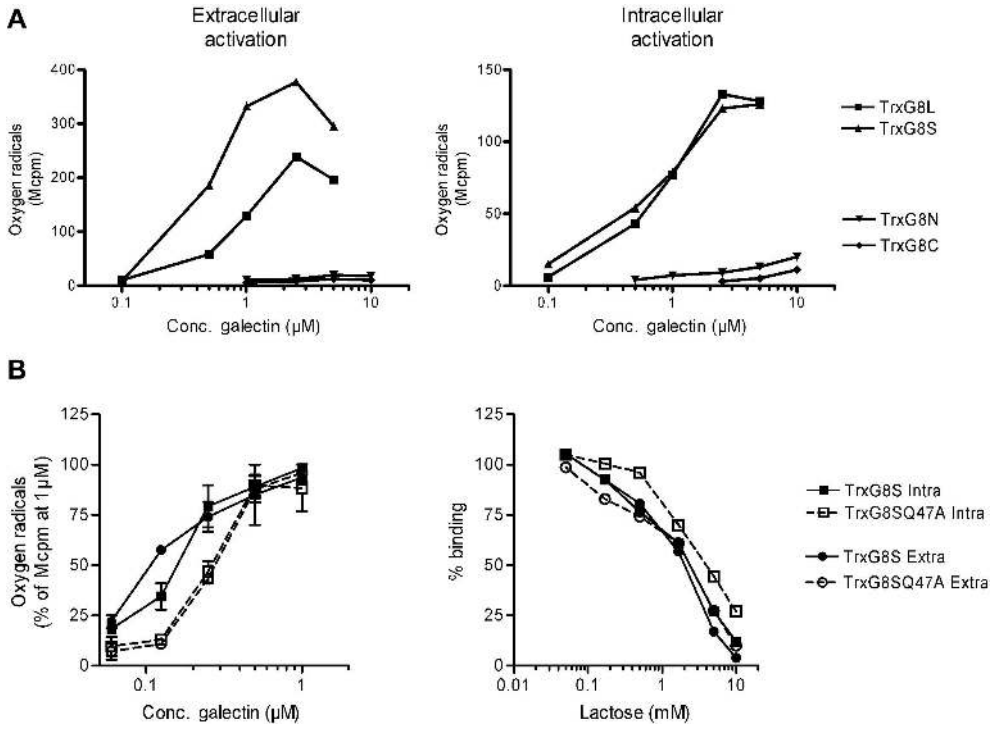

Fig. 5. Activation of NADPH-oxidase in neutrophils by galectin-8 and mutant TrxG8SQ47A. (**A**) Extracellular (left graph) and intracellular (right graph) activation of NADPH-oxidase in LPS-primed neutrophils by TrxG8S (▲), TrxG8L (■), TrxG8N (dtrif;), and TrxG8C (◆). Oxidative burst was measured by CL produced by reactive oxygen species and peak value plotted against the concentration of galectin used. One of four representative experiments is shown. (**B**) Dose–response of extracellular activation (•) and intracellular activation (□) of oxidative burst induced by TrxG8S (filled symbols, continuous line) or TrxG8SQ47A (open symbols, dashed line) is shown to the left. The graph includes data from three experiments where the response induced by 1 μM galectin in each experiment is set to 100%. Error bars represent the standard deviation. The right panel shows dose–response curves from lactose inhibition of oxidative burst induced by 1 μM galectin.

CRD acts on its own is raised by the discovery of possible regulatory cleavage of the linker (Nishi et al. 2006).

Materials and methods

Fluorescent probes and saccharides

The fluorescent probes are listed in Supplementary Table S2 with mass spectrometry (MS) and nuclear magnetic resonance (NMR) data for those previously unpublished. The syntheses of probes **2**, **14**, **15**, and **21** are detailed in Sorme et al. (2004). Probe **3** was synthesized using sialyltransferase analogously to **14**. The synthesis of probe **1** is detailed in Oberg et al. (2003), and probes **5**, **8**, **9**, **10**, **11**, **12**, **13**, **18**, **19**, **20**, **22**, **23**, and **24** were synthesized analogously to **1**. Probes **4**, **6**, **7**, **16**, and **17** were synthesized from unprotected saccharides equipped with a 2-azidoethyl aglycon, generously provided by Consortium for Functional Glycomics. The azide functionality was reduced with H_2 (1 atm) over Pd–C (5%) and the subsequent amide coupling of the crude amine with 5-carboxyfluorescein was carried out essentially as detailed in Oberg et al. (2003). Small saccharides used for inhibition were synthesized locally or obtained from Sigma (St Louis, MO).

Expression constructs

DNA encoding the gene of human galectin-8 or the separate domains were cloned into the pET-32 Ek/LIC vector (Novagen, Madison, WI) according to the manufacturer's instructions. Briefly, I.M.A.G.E. clone 2208156 (ATCC) was used as template together with the following polymerase chain reaction (PCR) primers: Gal-8 Fw: 5′-gac gac gac aag atg ATG TTG TCC TTA AAC AAC-3′, Gal-8 Rev: 5′-gag gag aag ccc ggt GGC TAC CAG CTC CTT ACT TCC A-3′, Gal-8 MidFw: 5′-gac gac gac aag atg CAG CTT AGC CTG CCA TTC GCT G-3′, and Gal-8 MidRev: 5′-gag gag aag ccc ggt TCA GTC CGA GCT GAA GCT AAA ACC-3′. Sequences needed for ligation-independent cloning (LIC) are underlined. The desired galectin-8 gene fragment was amplified using PCR and allowed to anneal with the pET-32 Ek/LIC vector, generating plasmids pTrxG8S (primers Gal-8 Fw and Gal-8 Rev), pTrxG8N (Gal-8 Fw and Gal-8 Mid Rev), and pTrxG8C (Gal-8 Mid Fw and Gal-8 Rev). A clone encoding the galectin-8 isoform with a long linker, containing the extra insertion IS1 (Bidon et al. 2001), was obtained by cleavage of pTrxG8S and I.M.A.G.E. clone 3922939 with *Bsm*I and *Mfe*I and subsequent ligation. Constructed vectors for galectin-8 short isoform (TrxG8S, Gal-8 amino acids 1-317), galectin-8 long isoform (TrxG8L, amino acids 1-359), galectin-8 N-terminal CRD (TrxG8N, amino acids 1-156), and galectin-8 C-terminal CRD (TrxG8C, amino acids 182-317) were used to transfect the host cell BL21 Star (DE3) (Invitrogen, San Diego, CA). All target proteins contains a $(His)_6$-tag and are expressed as a fusion with the highly soluble thioredoxin (Trx).

Mutants were generated using QuickChange® II Site-directed Mutagenesis Kit from Stratagene (San Diego, CA).

Template DNA (pTrxG8S or pTrxG8N) was transferred to and then isolated from *E. coli* XL1Blue (Stratagene). Mutagenic primers for the TrxG8S Q47A PCR were sense (5′-*gac gca gac aga ttc gcg gtg gat ctg cag aat ggc*-3′) and antisense (5′-*ctg cgt ctg tct aag cgc cac cta gac gtc tta ccg*-3′); and for the TrxG8N Y141S sense (5′-*gag aaa ata gac act ctg ggc att tct ggc aaa gtg aat att cac*-3′) and antisense (5′-*ctc ttt tat ctg tga gac ccg taa aga ccg ttt cac tta taa gag*-3′) (Invitrogen). Successful mutagenesis was confirmed by sequencing (GATC Biotech, Konstanz, Germany) in both forward and reverse direction. Mutated plasmids were then transferred to *Escherichia coli* BL21Star(DE3) (Novagen).

Expression and purification of recombinant galectins

All proteins produced in *E. coli* BL21 (DE3) Star were purified over a lactosyl-sepharose column (Massa et al. 1993) alone (TrxG8S, TrxG8L, and TrxG8N) or as a combination of both a Ni^{2+}-coupled column and lactosyl-sepharose column (TrxG8C). Enterokinase treatment of TrxG8N and separation using a Ni^{2+}-coupled column allowed purification of Trx alone.

Fusion of galectin-8 proteins with Trx resulted in expressed proteins of the estimated size having high solubility (up to 500 μM) (results not shown). The Trx-tag did not hinder lactose-binding activity as assayed by the binding to lactosyl-sepharose during purification. Cleavage of fusion proteins TrxG8S and TrxG8N with enterokinase (to remove Trx and its linker, Biozyme Laboratories, San Diego, CA) resulted in precipitation at concentrations above 0.5 mg/mL, i.e. 9 μM galectin-8S or 14 μM Gal-8N. G8C did not precipitate at concentrations up to 1 mg/mL (approximately 30 μM) (data not shown).

AlexaFluor and fluorescein labeling of recombinant galectins

Labeling of recombinant galectins with AlexaFluor488 was done using a kit from Molecular probes (Invitrogen) as instructed by the manufacturer. All reactions started with 1 mg galectin-8 thioredoxin fusion protein (TrxGal-8) in 1 mL phosphate-buffered saline (PBS; 118 mM NaCl, 63 mM Na/K-phopshate, pH 7.2) and were purified from unreacted Alexa-dye using desalting columns according to the manufacturer's instructions. Specific fluorescence intensity of labeled proteins indicated that TrxG8C incorporated fewer AlexaFluor molecules per galectin molecule than the other galectins (data not shown).

For fluorescein labeling, 2 mg of recombinant proteins were dissolved in 1 mL buffer (100 mM KH_2PO_4, pH 8.2). A stock solution of succinimide-activated fluorescein (20 mM) made in dimethyl sulfoxide was added to the protein solution in a molar ratio of 10:1 (fluorescein–protein) and the mixture incubated for 1 h at 37 °C. After incubation un-reacted succinimide–fluorescein was quenched with 100 μL of 1 M Tris–HCl for 30 min at room temperature (RT). Labeled protein was separated from the un-reacted fluorescein by a buffer change to PBS on a PD10 column (Amersham Biosciences, Uppsala, Sweden), and if necessary concentrated by spin-filter concentration. Fluorescence measurements on fluorescein-labeled galectins were used to calculate the number of fluorescein incorporated per protein molecule (0.5–1).

Glycan microarray

The glycan microarrays on glass microscope slides were printed on Nexterion Schott Type H slides (SCHOTT Nexterion, Louisville, KY) as previously described (Blixt et al. 2004). Recombinant galectins labeled with AlexaFluor488 and diluted to 200 and 40 μg/mL in Tris-buffered saline (20 mM Tris, 150 mM NaCl, pH 7.4) containing 2 mM $CaCl_2$, 2 mM $MgCl_2$, 1% bovine serum albumin (BSA), and 0.05% Tween-20 were used for analysis on the glycan microarray. An aliquot (70 μL) of each labeled galectin solution was applied to separate microarray slides and incubated under a coverslip for 60 min in a dark, humidified chamber at RT. After the incubation, the cover slips were gently removed in a solution of Tris-buffered saline containing 0.05% Tween-20 and washed by gently dipping the slides 4 times in successive washes of Tris-buffered saline containing 0.05% Tween-20, Tris-buffered saline, and deionized water. After the last wash, the slides were spun in a slide centrifuge for approximately 15 s to dry and immediately scanned in a ProScanArray MicroArray Scanner (PerkinElmer, Waltham, MS) using an excitation wavelength of 488 nm and ImaGene software (BioDiscovery, Inc., El Segundo, CA) to quantify fluorescence, reported as RFU. The maximum measurable value was 50 000 RFU. Each saccharide on the array is represented by six spots. The highest and lowest values were omitted, and the data are reported as the average of the reaming four.

Fluorescence anisotropy assay (fluorescence polarization)

Lactose was removed from the recombinant proteins by a buffer change to MEPBS using a desalting column (PD10) and followed by repeated dilutions with lactose-free buffer and spin-filter concentrations. The recombinant proteins were then mixed with fluorescein-labeled saccharides (probes) in a total volume of 180 or 200 μL. Final concentration of probes were held at 0.1 or 0.01 μM while concentration of protein ranged from 0.02 to 50 μM. Measurements were performed at RT as well as on chilled plates (about 4 °C). Analyses were performed using the instrument POLARstar (excitation 485 nm/emission 520 nm) with software FLUOstar Galaxy version 4.11-0 (BMG Lab-Technologies, Offenburg, Germany). To measure the affinity of soluble unlabeled saccharides, their potency as inhibitors was measured at a fixed concentration of galectin and probe as described (Sorme et al. 2004).

The value measured in the fluorescence polarization assay is reported as anisotropy (A) in units of *mA* (number of mA calculated as $A \times 1000$), which correlates directly with fraction of bound probe, as described in general by Lakowicz (1999) and for galectins by Sorme et al. (2004). From the curves of galectin concentration (x-axis) versus A (y-axis), A_0 and A_{max} were measured and K_d values were calculated (Sorme et al. 2004). For nonbinding probes (**21**–**24**), the anisotropy remained at A_0 (as for free probe) for all galectin concentrations demonstrating the lack of background signal in this assay. For binding probes, the plots start at a value corresponding to unbound probe (A_0) and, with increasing galectin concentration, approach a maximum value (A_{max}) corresponding to bound probe. The position of the curve along the x-axis reflects the affinity with the dissociation constant (K_d) being approximately equal to the concentration where half-maximal binding

is reached. A_{max} was determined, when possible, by adding high enough galectin concentration to reach near saturation of the probe. When the affinity of the galectin was too low for this, A_{max} was calculated by extrapolation of the binding curve from pairs of data points representing consecutive galectin concentrations, by solving the equation of mass action for a simple one-to-one interaction between galectin and probe for each data point. The K_d of inhibitors were calculated as described by Sorme et al. (2004).

The A_{max} is, as mentioned earlier, the anisotropy of the probe when bound to the galectin. It is determined mainly by two factors. Firstly, the tumbling of the galectin–probe complex, which is much slower than the free probe, therefore $A_{max} \gg A_0$. Secondly, the mobility of the fluorescein moiety independent of the rest of the probe (so called segmental motions or propeller effects, Lakowicz 1999), which reduces A_{max}. The rate of this independent movement and consequently the degree of anisotropy reduction depend on the local environment of the fluorescein moiety in the bound probe. Therefore, A_{max} also reflects how the probe is bound to the galectin.

Molecular modeling

A homology model was constructed for the N-terminal domain of human galectin-8 (amino acids 14-153 in NP 006490), based on the X-ray crystal structure of galectin-3 CRD with a bound LacNAc derivative (Seetharaman et al. 1998; Sorme et al. 2005), using Prime (Prime version 1.5, Macromodel version 9.1, Schrödinger, LLC, New York, NY, 2005). The loop near the galactose-binding site, between β-strands S4 and S5 (residue **71**–**77**) was further refined, also using Prime. The resulting structure was optimized using the Macromodel (Prime version 1.5) force-field MMFFS–water, after which a salt-bridge between Arg72 and Glu89 was present. Bound oligosaccharides were constructed from the preferred solution conformation of the saccharide, and the galactose occupying site C of the homology model was placed as in the crystal structure. The saccharide π, ψ angles, as well as the conformation of the Arg45 side chain, were manually adjusted to generate possible binding modes and the resulting complexes were optimized.

Flow cytometric measurements

A total of 10^6 cells of either U937 (a human monocytic cell line) or MOLT-4 (a human T-lymphoblast cell line), grown to a density of around 1×10^6 cells/mL in RPMI-1640 supplemented with 10% fetal calf serum, were washed twice with flow cytometry buffer (PBS, pH 7.2, supplemented with 1% (w/v) BSA). The cells were incubated with fluorescein-labeled galectins in a total volume of 100 μL for 30 min on ice. After incubation, flow cytometric analysis was performed using a FACSCalibur flow cytometer and CellQuest software (BD Biosciences). The cells were kept on ice throughout the experiment. Due to agglutination of cells, protein concentrations above 1 μM were not measured for F-TrxG8L or F-TrxG8S.

Lactose inhibition experiments were performed on U937 cells grown to a density of 0.5×10^6 cells/mL, incubated with a fixed protein concentration of 0.2 μM for F-TrxG8L and F-TrxG8S, 2 μM for F-TrxG8N and 5 μM for F-TrxG8C, and increasing amounts of lactose. Lactose concentrations were ranging from 0.005 to 100 mM.

In each experimental run, populations of beads containing known numbers of fluorescein molecules, the MESF kit (Bang Laboratories, Inc., Fishers, IN), were used for calibration. The beads provided an estimate of the number of fluorescein molecules per mean fluorescence intensity (MFI) unit. With this, the MFI of galectin-treated cells was used to calculate the number of bound galectin molecules per cell after correction for specific labeling of the galectins (fluorscein per protein molecule).

Calculation of theoretical lactose inhibition curves

Models of cell surface binding of galectin (Ga) were generated assuming presence of one or two receptors (R_1 and R_2) of different density and affinities (K_{dR_1} and K_{dR_2} in nM). The number of receptors per cell was converted to nanomolar concentrations ($[R_1]_{tot}$ and $[R_2]_{tot}$) in the sample, by multiplying by number of cells per liter and 10^9 followed by division by Avogadro's number. $[Ga]_{tot}$, was the total fixed concentration of galectin added in the particular experiment and, K_{dL}, the solution phase affinity of the galectin for lactose, was taken from the value obtained by testing inhibition in the fluorescence anisotropy assay. Under these assumptions, the sum of galectin bound to the one or two receptors was calculated for each of an exponential series of assumed lactose concentrations ($[L]_{tot}$).

The binding of galectin to the two receptors is governed by three equations of mass action:

$$K_{dR_1} = [R_1] \times [Ga]/[Ga][R_1Ga] \quad (1)$$

$$K_{dR_2} = [R_2] \times [Ga]/[Ga][R_2Ga] \quad (2)$$

$$K_{dL} = [L] \times [Ga]/[LGa] \quad (3)$$

The amount of bound galectin is obtained by solving each of these equations. For example, galectin bound to R_1 will be

$$[R_1Ga] = T_1/2 - (T_1^2/4 - S_1)^{1/2} \quad (4)$$

where $T_1 = [Ga]_{tot} + [R_1]_{tot} + K_{dR_1} - [R_2Ga] - [LGa]$ and $S_1 = [R_1]_{tot} \times ([Ga]_{tot} - [R_2Ga] - [LGa])$ with suffix "tot" indicating total concentration.

The equations for galectin bound to R_2 (equation 2) and lactose (equation 3) have the same form with $T_2 = [Ga]_{tot} + [R_2]_{tot} + K_{dr_2} - [R_1Ga] - [LGa]$ and $S_2 = [R_2]_{tot} \times ([Ga]_{tot} - [R_1Ga] - [LGa])$, and $T_L = [Ga]_{tot} + [L]_{tot} + K_{dL} - [R_1Ga] - [R_2Ga]$ and $S_L = [L]_{tot} \times ([Ga]_{tot} - [R_1Ga] - [R_2Ga])$, respectively.

The solution to the three equation system was approached by an iterative process. In this, the receptor binding was first calculated in the absence of lactose by solving equation (1), assuming that the unknown $[R_2Ga] = 0$ (needed to calculate T_1 and S_1), followed by solving equation (2). Then equation (1) was solved again, now entering the just calculated value for $[R_2Ga]$, followed by solution of equation (2) again. This loop was repeated 4 times.

Then the receptor binding in the presence of inhibitor was calculated by first solving equation (3) to obtain $[LGa]$. For

this, the values of $[R_2Ga]$ and $[R_1Ga]$ were taken from the previous calculation at the nearest lower lactose concentration, or for the first inhibitor concentration from the binding in the absence of lactose. Then equations (1) and (2) were solved, and the loop of equations (3), (1), and (2) was started again. In each case, the most recently calculated values were used for $[R_1Ga]$, $[R_2Ga]$, and [LGa]. The loop was repeated 4 times. The convergence of the calculation was monitored by comparing the calculated values with those from the previous iteration. Already after four iterations, the change was $<1\%$.

NA treatment

A total of 7.5×10^6 cells of either U937 or MOLT-4 was washed and resuspended in 0.5 mL RPMI-1640 medium. A 100 mU of NA from *Vibrio cholerae* (E.C. 3.2.1.18) or an α2,3-specific recombinant NA was added, and the cells were incubated for 2 h at 37 °C. After incubation, the cells were exposed to F-TrxG8L (0.2 μM), F-TrxG8S (0.2 μM), F-TrxG8N (2 μM), F-TrxG8C (5 μM), fluorescein-tagged SNA (5 μg/mL, Vector Laboratories, Burlingame, CA), or MAL II (biotinylated MAL II, 40 μg/mL, preincubated with FITC-streptavidin 25:1, Vector Laboratories) and analyzed with flow cytometry.

Isolation and priming of neutrophils

Human neutrophils were isolated as described by Boyum (1968) from buffy coats from healthy volunteers, using dextran sedimentation and Ficoll–Paque gradient centrifugation. The cells were resuspended in Krebs–Ringer phosphate buffer containing glucose (10 mM), Ca^{2+} (1 mM), and Mg^{2+} (1.5 mM) (pH 7.3) and stored on ice until use. Cells were primed with LPS as described (Almkvist et al. 2001) or TNFα (Bylund et al. 2004).

Measurement of NADPH-oxidase activity by chemiluminescence

The NADPH-oxidase activity was measured using luminol/isoluminol-amplified chemiluminescence (CL; Dahlgren and Karlsson 1999). The CL was measured in a Biolumat LB 9505 (Berthold Co., Bad Wildbad, Germany) using polypropylene tubes with a 900 μL reaction mixture containing 10^6 neutrophils. The tubes were equilibrated for 5 min in the Biolumat at 37°C, before the addition of 100 μL of TrxGal-8 protein. The light emission was recorded continuously. To quantify the intracellularly and extracellularly generated reactive oxygen species, respectively, two different reaction mixtures were used. The extracellular release of superoxide anion was measured in tubes containing neutrophils, horseradish peroxidase (a cell impermeable peroxidase; 4 U), and isoluminol (a cell impermeable CL substrate; 6×10^{-5} M). The intracellular production of reactive oxygen species was measured in tubes containing neutrophils, superoxide dismutase (a cell impermeable scavenger for O_2; 50 U), catalase (a cell impermeable scavenger for H_2O_2; 2000 U), and luminol (a cell permeable CL substrate; 2×10^{-5} M).

Supporting information

Table S1a–d lists results from glycan array including structural information of printed saccharides, RFU values from experiments with both 200 g/mL and 40 μg/mL and their standard deviations. Table S1a represents TrxG8N; S1b, TrxG8C; S1c, TrcG8S and S1d TrxG8L. Table S2 depicts and lists the fluorescent probes used with mass spectrometry and NMR data for those previously unpublished.

Supplementary data

Supplementary data are available at Glycobiology online (http://glycob.oxfordjournals.org/).

Acknowledgments

We thank Barbro Kahl-Knutsson, Inga Svensson-Danielsson and Veronica Johansson for excellent laboratory assistance, Prof. Eric Fillion for collaborating on fluorescein conjugation. The precursors for probes and support to DS and RDC were provided by the Consortium for Functional Glycomics NIH Grant GM62116 and an NIH Grant P01 HL085607-01 to RDC. The work was sponsored by the Swedish Foundation for Strategic Research and the Swedish Research Council. This project was also supported by the programs 'Glycoconjugates in Biological Systems' and 'Chemistry for the Life Sciences' sponsored by the Swedish Foundation for Strategic Research.

Conflict of interest statement

None declared.

Abbreviations

BSA, bovine serum albumin; CL, chemiluminescence; CRD, carbohydrate recognition domain; CHO, Chinese hamster ovary; Gal-8C, C-terminal CRD of galectin-8; Gal-8L, galactin-8 isoform with long linker; Gal-8N, N-terminal CRD of galctin-8; Gal-8S, galectin-8 isoform with short linker; Lac, lactose; LacNAc, *N*-acteyl lactoseamine; LIC, ligation-independent cloning; LNT, lacto-*N*-triose; LNnT, Lacto-*N*-neotetraose; LPS, lipopolysaccharide; MAL II, *Maackia amurensis* lectin II; MFI, mean fluorescence intensity; NA, neuraminidase; PBS, phosphate-buffered saline; PCR, polymerase chain reaction; RFU, relative fluorescence units; RT, room temperature; SA, sialic acid; SNA, *Sambucus nigra* agglutinin; TNFa, tumor necrosis factor alpha; TrxG8C, thioredoxin fusion protein of Gal-8C; TrxG8L, thioredoxin fusion protein of Gal-8L; TrxG8N, thioredoxin fusion protein of Gal-8N; TrxG8S, thioredoxin fusion protein of Gal-8S

References

Almkvist J, Dahlgren C, Leffler H, Karlsson A. 2002. Activation of the neutrophil nicotinamide adenine dinucleotide phosphate oxidase by galectin-1. J Immunol. 168:4034–4041.

Almkvist J, Dahlgren C, Leffler H, Karlsson A. 2004. Newcastle disease virus neuraminidase primes neutrophils for stimulation by galectin-3 and formyl-Met-Leu-Phe. Exp Cell Res. 298:74–82.

Almkvist J, Faldt J, Dahlgren C, Leffler H, Karlsson A. 2001. Lipopolysaccharide-induced gelatinase granule mobilization primes neutrophils for activation by galectin-3 and formylmethionyl-Leu-Phe. Infect Immun. 69:832–837.

Barondes SH, Castronovo V, Cooper DN, Cummings RD, Drickamer K, Feizi T, Gitt MA, Hirabayashi J, Hughes C, Kasai K, et al. 1994. Galectins: a family of animal beta-galactoside-binding lectins. Cell. 76:597–598.

Bidon N, Brichory F, Hanash S, Bourguet P, Dazord L, Le Pennec JP. 2001. Two messenger RNAs and five isoforms for Po66-CBP, a galectin-8 homolog in a human lung carcinoma cell line. Gene. 274:253–262.

Blixt O, Head S, Mondala T, Scanlan C, Huflejt ME, Alvarez R, Bryan MC, Fazio F, Calarese D, Stevens J, et al. 2004. Printed covalent glycan array for ligand profiling of diverse glycan binding proteins. Proc Natl Acad Sci USA. 101:17033–17038.

Boyum A. 1968. Isolation of mononuclear cells and granulocytes from human blood. Isolation of monuclear cells by one centrifugation, and of granulocytes by combining centrifugation and sedimentation at 1 g. Scand J Clin Lab Invest Suppl. 97:77–89.

Brewer CF. 2002. Binding and cross-linking properties of galectins. Biochim Biophys Acta. 1572:255–262.

Bylund J, Pellme S, Fu H, Mellqvist UH, Hellstrand K, Karlsson A, Dahlgren C. 2004. Cytochalasin B triggers a novel pertussis toxin sensitive pathway in TNF-alpha primed neutrophils. BMC Cell Biol. 5:21.

Cabrera PV, Amano M, Mitoma J, Chan J, Said J, Fukuda M, Baum LG. 2006. Haploinsufficiency of C2GnT-I glycosyltransferase renders T lymphoma cells resistant to cell death. Blood. 108:2399–2406.

Carcamo C, Pardo E, Oyanadel C, Bravo-Zehnder M, Bull P, Caceres M, Martinez J, Massardo L, Jacobelli S, Gonzalez A, et al. 2006. Galectin-8 binds specific beta1 integrins and induces polarized spreading highlighted by asymmetric lamellipodia in Jurkat T cells. Exp Cell Res. 312:374–386.

Collins BE, Paulson JC. 2004. Cell surface biology mediated by low affinity multivalent protein–glycan interactions. Curr Opin Chem Biol. 8: 617–625.

Dahlgren C, Karlsson A. 1999. Respiratory burst in human neutrophils. J Immunol Methods. 232:3–14.

Danielsen EM, Hansen GH. 2006. Lipid raft organization and function in brush borders of epithelial cells. Mol Membr Biol. 23:71–79.

Delacour D, Cramm-Behrens CI, Drobecq H, Le Bivic A, Naim HY, Jacob R. 2006. Requirement for galectin-3 in apical protein sorting. Curr Biol. 16: 408–414.

Delacour D, Gouyer V, Zanetta JP, Drobecq H, Leteurtre E, Grard G, Moreau-Hannedouche O, Maes E, Pons A, Andre S, et al. 2005. Galectin-4 and sulfatides in apical membrane trafficking in enterocyte-like cells. J Cell Biol. 169:491–501.

Hadari YR, Arbel-Goren R, Levy Y, Amsterdam A, Alon R, Zakut R, Zick Y. 2000. Galectin-8 binding to integrins inhibits cell adhesion and induces apoptosis. J Cell Sci. 113(Pt 13):2385–2397.

Hernandez JD, Nguyen JT, He J, Wang W, Ardman B, Green JM, Fukuda M, Baum LG. 2006. Galectin-1 binds different CD43 glycoforms to cluster CD43 and regulate T cell death. J Immunol. 177:5328–5336.

Hirabayashi J, Hashidate T, Arata Y, Nishi N, Nakamura T, Hirashima M, Urashima T, Oka T, Futai M, Muller WE, et al. 2002. Oligosaccharide specificity of galectins: a search by frontal affinity chromatography. Biochim Biophys Acta. 1572:232–254.

Houzelstein D, Goncalves IR, Fadden AJ, Sidhu SS, Cooper DN, Drickamer K, Leffler H, Poirier F. 2004. Phylogenetic analysis of the vertebrate galectin family. Mol Biol Evol. 21:1177–1187.

Ideo H, Seko A, Ishizuka I, Yamashita K. 2003. The N-terminal carbohydrate recognition domain of galectin-8 recognizes specific glycosphingolipids with high affinity. Glycobiology. 13:713–723.

Ilarregui JM, Bianco GA, Toscano MA, Rabinovich GA. 2005. The coming of age of galectins as immunomodulatory agents: impact of these carbohydrate binding proteins in T cell physiology and chronic inflammatory disorders. Ann Rheum Dis. 64(Suppl 4):iv96–103.

Jencks WP. 1981. On the attribution and additivity of binding energies. Proc Natl Acad Sci USA. 78:4046–4050.

Karlsson A, Follin P, Leffler H, Dahlgren C. 1998. Galectin-3 activates the NADPH-oxidase in exudated but not peripheral blood neutrophils. Blood. 91:3430–3438.

Kiessling LL, Gestwicki JE, Strong LE. 2006. Synthetic multivalent ligands as probes of signal transduction. Angew Chem Int Ed Engl. 45:2348–2368.

Lakowicz JR. 1999. Principles of fluorescence spectroscopy. New York: Kluwer Academic/Plenum Publishers.

Landersjo C, Jansson JL, Maliniak A, Widmalm G. 2005. Conformational analysis of a tetrasaccharide based on NMR spectroscopy and molecular dynamics simulations. J Phys Chem B Condens Matter Mater Surf Interfaces Biophys. 109:17320–17326.

Lee RT, Lee YC. 2000. Affinity enhancement by multivalent lectin–carbohydrate interaction. Glycoconj J. 17:543–551.

Lee YC, Townsend RR, Hardy MR, Lonngren J, Arnarp J, Haraldsson M, Lonn H. 1983. Binding of synthetic oligosaccharides to the hepatic Gal/GalNAc lectin. Dependence on fine structural features. J Biol Chem. 258:199–202.

Leffler H, Barondes SH. 1986. Specificity of binding of three soluble rat lung lectins to substituted and unsubstituted mammalian beta-galactosides. J Biol Chem. 261:10119–10126.

Leffler H, Carlsson S, Hedlund M, Qian Y, Poirier F. 2004. Introduction to galectins. Glycoconj J. 19:433–440.

Leppanen A, Stowell S, Blixt O, Cummings RD. 2005. Dimeric galectin-1 binds with high affinity to alpha2,3-sialylated and non-sialylated terminal *N*-acetyllactosamine units on surface-bound extended glycans. J Biol Chem. 280:5549–5562.

Levy Y, Arbel-Goren R, Hadari YR, Eshhar S, Ronen D, Elhanany E, Geiger B, Zick Y. 2001. Galectin-8 functions as a matricellular modulator of cell adhesion. J Biol Chem. 276:31285–31295.

Levy Y, Auslender S, Eisenstein M, Vidavski RR, Ronen D, Bershadsky AD, Zick Y. 2006. It depends on the hinge: a structure-functional analysis of galectin-8, a tandem-repeat type lectin. Glycobiology. 16:463–476.

Liu FT, Rabinovich GA. 2005. Galectins as modulators of tumour progression. Nat Rev Cancer. 5:29–41.

Lobsanov Y, Gitt M, Leffler H, Barondes S, Rini J. 1993. X-ray crystal structure of the human dimeric S-Lac lectin, L-14-II, in complex with lactose at 2.9-A resolution. J Biol Chem. 268:27034–27038.

Lu LH, Nakagawa R, Kashio Y, Ito A, Shoji H, Nishi N, Hirashima M, Yamauchi A, Nakamura T. 2006. Characterization of galectin-9-induced death of Jurkat T-Cells. J Biochem (Tokyo) 141:157–172.

Massa SM, Cooper DN, Leffler H, Barondes SH. 1993. L-29, an endogenous lectin, binds to glycoconjugate ligands with positive cooperativity. Biochemistry. 32:260–267.

Mehta P, Cummings RD, McEver RP. 1998. Affinity and kinetic analysis of P-selectin binding to P-selectin glycoprotein ligand-1. J Biol Chem. 273: 32506–32513.

Murray CW, Verdonk ML. 2002. The consequences of translational and rotational entropy lost by small molecules on binding to proteins. J Comput Aided Mol Des V16:741–753.

Nishi N, Itoh A, Shoji H, Miyanaka H, Nakamura T. 2006. Galectin-8 and galectin-9 are novel substrates for thrombin. Glycobiology. 16:15C–20C.

Nishi N, Shoji H, Seki M, Itoh A, Miyanaka H, Yuube K, Hirashima M, Nakamura T. 2003. Galectin-8 modulates neutrophil function via interaction with integrin alphaM. Glycobiology. 13:755–763.

Oberg CT, Carlsson S, Fillion E, Leffler H, Nilsson UJ. 2003. Efficient and expedient two-step pyranose-retaining fluorescein conjugation of complex reducing oligosaccharides: galectin oligosaccharide specificity studies in a fluorescence polarization assay. Bioconjug Chem. 14: 1289–1297.

Patnaik SK, Potvin B, Carlsson S, Sturm D, Leffler H, Stanley P. 2006. Complex N-glycans are the major ligands for galectin-1, -3, and -8 on Chinese hamster ovary cells. Glycobiology. 16:305–317.

Rauvala H, Finne J. 1979. Structural similarity of the terminal carbohydrate sequences of glycoproteins and glycolipids. FEBS Lett 97:1–8.

Rini JM. 1995. Lectin structure. Annu Rev Biophys Biomol Struct. 24: 551–577.

Seetharaman J, Kanigsberg A, Slaaby R, Leffler H, Barondes SH, Rini JM. 1998. X-ray crystal structure of the human galectin-3 carbohydrate recognition domain at 2.1-A resolution. J Biol Chem. 273:13047–13052.

Somers WS, Tang J, Shaw GD, Camphausen RT. 2000. Insights into the molecular basis of leukocyte tethering and rolling revealed by structures of P- and E-selectin bound to SLe(X) and PSGL-1. Cell. 103:467–479.

Sorme P, Arnoux P, Kahl-Knutsson B, Leffler H, Rini JM, Nilsson UJ. 2005. Structural and thermodynamic studies on cation–pi interactions in lectin–ligand complexes: high-affinity galectin-3 inhibitors through fine-tuning of an arginine–arene interaction. J Am Chem Soc. 127:1737–1743.

Sorme P, Kahl-Knutsson B, Huflejt M, Nilsson UJ, Leffler H. 2004. Fluorescence polarization as an analytical tool to evaluate galectin–ligand interactions. Anal Biochem. 334:36–47.

Stillman BN, Hsu DK, Pang M, Brewer CF, Johnson P, Liu FT, Baum LG. 2006. Galectin-3 and galectin-1 bind distinct cell surface glycoprotein receptors to induce T cell death. J Immunol. 176:778–789.